Journal of Constructional Steel Research 70 (2012) 350–357

Contents lists available at SciVerse ScienceDirect

Journal of Constructional Steel Research

Elasto–plastic analysis of steel plane frames using Homotopy Perturbation Method

H. Saffari [a,*], I. Mansouri [a], M.H. Bagheripour [a], H. Dehghani [b]

[a] Department of Civil Engineering, Shahid Bahonar University of Kerman, P.O. Box 76169133, Kerman, Iran
[b] Department of Civil Engineering, Islamic Azad University–Bam Branch, P.O. Box 76615-184, Bam, Iran

ARTICLE INFO

Article history:
Received 24 March 2011
Accepted 10 October 2011
Available online 16 November 2011

Keywords:
Plane frame
Homotopy Perturbation Method (HPM)
Newton-iterative method
Plastic hinge

ABSTRACT

In this research a new nonlinear method is developed based on Homotopy Perturbation Method (HPM) and is applied to elasto-plastic analysis of steel plane frames. The Homotopy algorithm can be considered as an advancement into classical methods of numerical computation such as Newton–Raphson method. In perturbation methods, perturbation quantities are used to transfer a nonlinear problem into a number of manageable linear sub-problems. Then an approximate solution is reached by summing up the results of first several sub-problems. The HPM developed here is applied to plane frames in which elastic–perfectly plastic behavior is assumed for structural material while conventional plastic hinges of zero length are used to model plasticity effect. Numerical examples are presented in this paper to show the accuracy and effectiveness of the proposed approach. Results obtained showed that when developed HPM is used for elasto-plastic analysis of structures, using various yield criteria for steel elements, less iteration is required to reach solution, and convergence is achieved very fast compared with conventional Newton–Raphson method.

1. Introduction

In recent years, nonlinear analysis has emerged as a replacement for linear analysis in many structural engineering problems. The growth in computers' processing speed and capacity has increased tendency towards more accurate solutions even for highly complex analysis methods.

For three decades now, nonlinear elastic and inelastic analysis of frame structures has been given attention by researchers. The methods for large deformation and stability analysis of elastic–plastic frames based on Eulerian formulation were introduced by Kassimali et al. [1–3].

The numerical method constitutes one of the most important aspects in the nonlinear analysis of structures. Newton–Raphson method, displacement control methods, Perturbation Method (PM) [4], self-correcting incremental procedure [4,5], the incremental stiffness procedure [5] and the initial value approach are commonly used for solution of nonlinear problems.

Papadrakakis and Gantes [6] used procedures for the solution of large-scale nonlinear equations applied to given trusses. Saffari et al. [7] introduced a new algorithm for nonlinear analysis of space trusses which reduced the number of iterations and hence the computational time. Papadrakakis [8] used two vector iteration methods in large deflection analysis of spatial structures. Crisfield [9] introduced an additional equation to the original stiffness equations for the arc-length control of tracing the equilibrium path. Recently, Saffari and Mansouri [10] have presented a new approach for nonlinear analysis of structures which accelerates the convergence rate. Tabatabaei et al. [11] applied a new iterative algorithm based on displacement control method, flow path normal, in nonlinear static analysis of frames.

Recently, singular perturbation techniques are considered as a suitable theoretical procedure in applied mechanics [12]. Analytical techniques such as the homotopy analysis method introduced by Liao [13,14] have shown their validity for highly nonlinear problems. However, the efficiency and applicability of the method to the structural analysis has yet to be examined.

More recently, computational and analytical methods based on the theory of homotopy have been given attention in applied mathematics. With the advent of modern computers, the theory has re-emerged as the foundation for a new class of numerical techniques known as the homotopy continuation method [15–17]. The advance in symbolic computation has empowered development of the homotopy method to provide analytical solutions for nonlinear equations [13]. Golbabai and Javidi [18] proposed an iterative method for solving systems of two nonlinear equations based on HPM. Although the method reduced the number of iterations required, convergence time was not satisfactory. Moreover, the Newton-like and perturbation method developed by Golbabai and Javidi [18] was used only for solution of nonlinear equations in applied mathematics problems and was limited to the system of 2×2 equations. No application, however, was shown to the structural analysis.

* Corresponding author. Tel.: +98 9131411509; fax: +98 3413220054.
E-mail addresses: hsaffari@mail.uk.ac.ir (H. Saffari), im_pce@yahoo.com (I. Mansouri), bagheri@mail.uk.ac.ir (M.H. Bagheripour), hdehghani@iaubam.ac.ir (H. Dehghani).

0143-974X/$ – see front matter © 2011 Elsevier Ltd. All rights reserved.
doi:10.1016/j.jcsr.2011.10.013

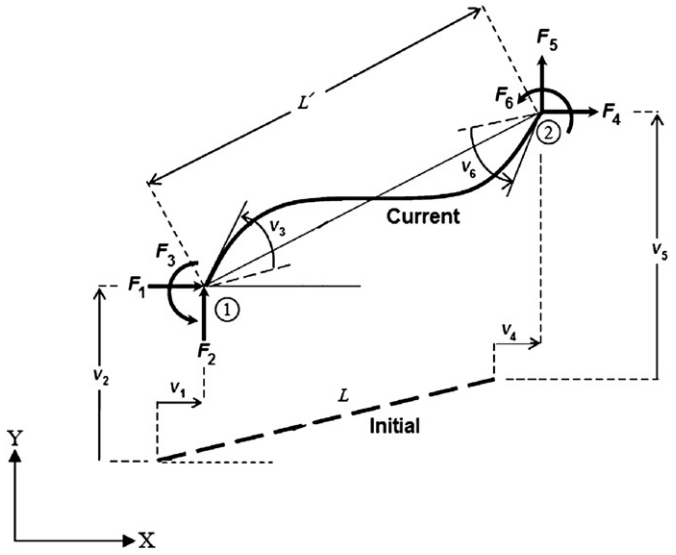

Fig. 1. Member forces and deformations in global coordinates.

Most of the methods for solving the nonlinear system of equations are time-consuming and expensive in the case of nonlinear analysis of complex structures, and many of them diverge during passing the limit points. The reason for these disadvantages is that in structures with complex behavior, the load–displacement curve is a sequence of softening and hardening states with limit points. Therefore, nonlinear analysis of such structures is often impossible by simple incremental iterative methods. The simple incremental iterative methods are conducted in successive load increments or displacements increments. Since the load level is constant in load increment method, passing the limit points is not possible and, hence, more efficient techniques are needed.

In this paper, an algorithm based on homotopy is designed to improve efficiency and accuracy of nonlinear analysis. The Newton-like and perturbation method developed by Golbabai and Javidi [18] for solution of limited system of nonlinear equations in applied mathematics is considered here. Based on Homotopy analysis the method is modified, reformulated and is also extended for large system of nonlinear equations as required in structural analysis. The method developed here is applied for engineering problems such as nonlinear structural analysis of plane frames. Crisfield method [9] is applied in order to pass the limit points. Newton–Raphson method is used in the phase of modifying iterations. The proposed method accelerates this phase of analysis. As will be shown, application of the algorithm efficiently reduces the number of iterations and hence the computational time for nonlinear analysis of steel plane frames with different plastic hinge type.

2. Geometrical nonlinear analysis of plane frame

2.1. Member force–deformation relation

Fig. 1 shows a beam-column element of length L, cross-sectional area A, moment inertia of section I and modulus of elasticity E, subjected to member end forces in global coordinates: $\{F\}=\{F_1\ F_2 F_3\ F_4 F_5\ F_6\}^T$.

For the plane frame member in its initial configuration, the global nodal coordinates are defined as (X_1, Y_1) for node 1 and (X_2, Y_2) for node 2 while in its current configuration, the coordinates are defined by $(X_1+V_1,\ Y_1+V_2)$ and $(X_2+V_4,\ Y_2+V_5)$ for node 1 and 2, respectively.

In Fig. 2 a plane frame member is shown subjected to member forces in local coordinates. These forces cause an axial deflection δ, and end rotations θ_1 and θ_2 at the ends 1 and 2, respectively. The

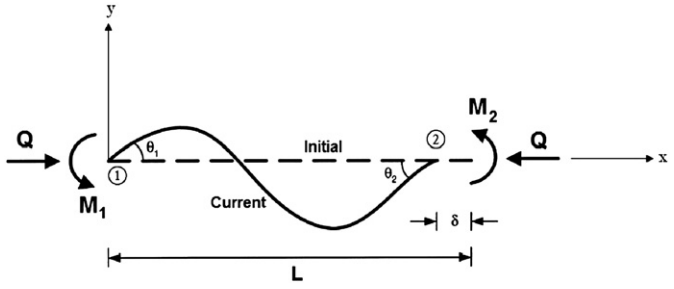

Fig. 2. Member forces and deformations in local coordinates.

sign conventions for forces and displacements are also shown in Fig. 2.

The slope-deflection equations for this member are;

$$M_1=\frac{EI}{L}(c_1\theta_1+c_2\theta_2),\qquad M_2=\frac{EI}{L}(c_2\theta_1+c_1\theta_2) \tag{1}$$

The element axial force Q can be expressed as [2]:

$$Q=AE\left[\frac{\delta}{L}-b_1(\theta_1+\theta_2)^2-b_2(\theta_1-\theta_2)^2\right] \tag{2}$$

in which c_1 and c_2 are the stability functions. For the state of compression, these functions are given by [2]:

$$c_1=\frac{\varphi(\sin\varphi-\varphi\cos\varphi)}{2(1-\cos\varphi)-\varphi\sin\varphi}\quad,\quad c_2=\frac{\varphi(\varphi-\sin\varphi)}{2(1-\cos\varphi)-\varphi\sin\varphi} \tag{3}$$

$$\varphi^2=\frac{QL^2}{EI}=\pi^2 q \tag{4}$$

where φ and q are parameters expressing the influence of the axial load on the element stiffness. Similarity, for tensile loads, the stability functions are obtained as [2]:

$$c_1=\frac{\psi(\sinh\psi-\psi\cosh\psi)}{2(\cosh\psi-1)-\psi\sinh\psi}\quad,\quad c_2=\frac{\psi(\psi-\sinh\psi)}{2(\cosh\psi-1)-\psi\sinh\psi} \tag{5}$$

$$\psi^2=-\frac{QL^2}{EI}=-\pi^2 q \tag{6}$$

c_1 and c_2 are inter-related by bowing functions. b_1 and b_2 are expressed as:

$$b_1=\frac{(c_1+c_2)(c_2-2)}{8\pi^2 q}\quad,\quad b_2=\frac{c_2}{8(c_1+c_2)}\ . \tag{7}$$

For members free of axial force, the stability functions c_1 and c_2 are reduced to constants as $c_1=4$ and $c_2=2$.

2.2. Equilibrium equation

The equilibrium equation for the structure can be written as:

$$f_i(x_1,x_2,\ .....,x_n)=P_i \tag{8}$$

where $\{x\}=\{x_1,x_2,\ldots,x_n\}^T$ denotes the vector of generalized coordinates formed from translations of nodes, $\{f\}$ is the vector of resultant internal forces which is a highly nonlinear function of $\{x\}$. The load–deflection relations show that it is almost impossible to explicitly

solve these equations. For computational purpose, it is useful to apply the differential form of the equation:

$$\{\Delta x\} = [\tau]^{-1}\{\Delta P\} \tag{9}$$

in which $\{\Delta x\}$ stands for incremental displacements, $\{\Delta P\}$ represents load increments, and $[\tau] = \left[\frac{\partial f_i}{\partial x_j}\right]$ constitutes the system tangent stiffness matrix which is explained in the following.

2.3. Tangent stiffness matrix

The stiffness matrix considered and used here is based on Eulerian beam-column theory [19]. The nodal force–displacement relationship is defined using a global stiffness matrix which is assembled from the element stiffness matrices. The member tangent stiffness matrix in local coordinates, $[t]$ is expressed by the following relation:

$$t_{ij} = \frac{\partial S_i}{\partial d_j} + \frac{\partial S_i}{\partial q}\cdot\frac{\partial q}{\partial d_j}, \qquad i,j = 1,2,3 \tag{10}$$

in which $S_1 = M_1, S_2 = M_2, S_3 = Q, d_1 = \theta_1, d_2 = \theta_2$ and $d_3 = \delta$. Substituting these parameters into Eq. (10), the equilibrium equation can be written as:

$$\begin{bmatrix} M_1 \\ M_2 \\ Q \end{bmatrix} = \frac{EI}{L}\begin{bmatrix} c_1 + \frac{G_1^2}{\pi^2 H} & c_2 + \frac{G_1 G_2}{\pi^2 H} & \frac{G_1}{LH} \\ c_2 + \frac{G_1 G_2}{\pi^2 H} & c_1 + \frac{G_2^2}{\pi^2 H} & \frac{G_2}{LH} \\ \frac{G_1}{LH} & \frac{G_2}{LH} & \frac{\pi^2}{L^2 H} \end{bmatrix}\begin{bmatrix} \theta_1 \\ \theta_2 \\ \delta \end{bmatrix} \tag{11}$$

in which:

$$G_1 = \frac{\partial c_1}{\partial q}\theta_1 + \frac{\partial c_2}{\partial q}\theta_2, \qquad G_2 = \frac{\partial c_2}{\partial q}\theta_1 + \frac{\partial c_1}{\partial q}\theta_2 \tag{12}$$

and

$$H = \frac{\pi^2 I}{L^2 A} + \frac{\partial b_1}{\partial q}(\theta_1 + \theta_2)^2 + \frac{\partial b_2}{\partial q}(\theta_1 - \theta_2)^2. \tag{13}$$

The global tangent stiffness matrix, $[\tau]$, is obtained by transferring local coordinates into the global coordinate. A detailed discussion on calculation of $[\tau]$ is provided in reference [2].

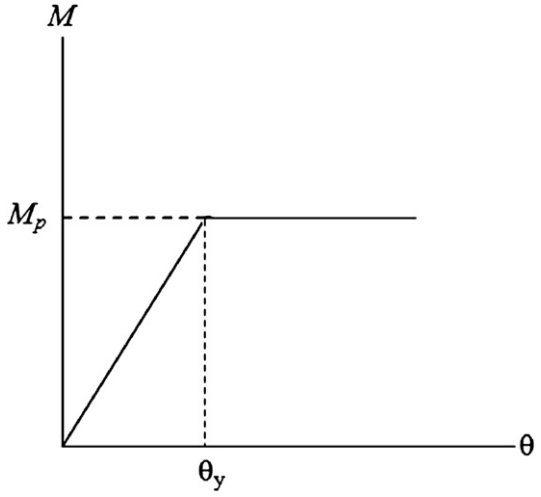

Fig. 3. Material behavior.

3. Elastic perfectly–plastic material

A perfectly plastic material associated with plastic hinge concept is used in this study to consider material non-linearity effect. In an elastic perfectly–plastic material, the effects of strain hardening are disregarded. It further implies that once the yield moment M_p is reached, the material yields and cannot withstand further stress. Such a behavior is schematically shown in Fig. 3 for elastic perfectly–plastic material.

It is of note that M_p (yield moment) is commonly defined by a yield criterion. Variety of yield criteria defining M_p has been introduced in structural engineering. In this paper, four yield criteria considering bending moment and axial force interaction are used these yield criteria are use for steel elements. These criteria and their corresponding descriptive relations are shown below:

a) Bilinear formula commonly used is expressed as [2]:

$$M_{pc} = \begin{cases} M_p & \text{for } \frac{|Q|}{Q_y} \le 0.15 \\ 1.18M_p\left(1 - \frac{|Q|}{Q_y}\right) & \text{for } \frac{|Q|}{Q_y} > 0.15 \end{cases}. \tag{14}$$

b) Simple criterion which is a linear relation between moment and axial force and is expressed as follows [20]:

$$M_{pc} = M_p\left(1 - \frac{|Q|}{Q_y}\right). \tag{15}$$

c) Quadratic relation between moment and axial force which is described by the following relation [20]:

$$M_{pc} = M_p\left(1 - \left(\frac{|Q|}{Q_y}\right)^2\right). \tag{16}$$

d) AISC–LRFD criterion which is quoted below [21]:

$$M_{pc} = \begin{cases} M_p\left(1 - \frac{|Q|}{2Q_y}\right) & \text{for } \frac{|Q|}{Q_y} < 0.2 \\ \frac{9}{8}M_p\left(1 - \frac{|Q|}{Q_y}\right) & \text{for } \frac{|Q|}{Q_y} \ge 0.2 \end{cases}. \tag{17}$$

In the above relations, M_p is full plastic moment capacity in the absence of axial force (equal to $Z.F_y$); M_{pc} represents reduced plastic moment capacity in the presence of axial force ($Q_y = A.F_y$); where F_y denotes yield stress, and Z stands for plastic modulus.

These criteria are schematically shown in Fig. 4 which provides a base of graphical comparison in a non-dimensional coordinates.

It should be noted that in inelastic analysis, the tangent stiffness matrix introduced in Section 2.3 has to be modified. A detailed discussion on the inelastic analysis can be found in [2].

4. Nonlinear analysis algorithm

4.1. Newton–Raphson method

General Newton–Raphson method is one of the numerical methods for iterative solution of nonlinear equations. In this method, an approximate solution is initially assumed to which an unknown value is subsequently added as a correcting factor to improve the initial solution. Using Taylor series, a system of nonlinear equations can be transformed into a linear form, the solution of which provides the necessary correcting factors to achieve an improved state of the

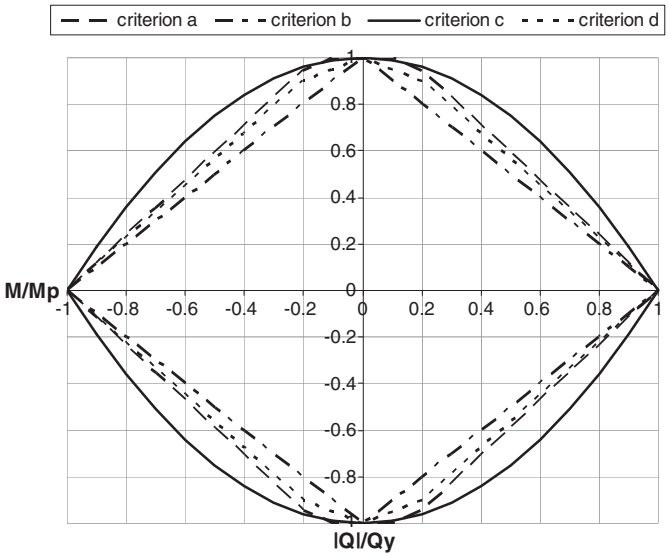

Fig. 4. Various types of yield criteria.

solution. This process is continued or repeated until convergence is reached within an acceptable tolerance [22,23].

4.2. Conjugate gradient (CG) method

The problem of solving nonlinear equations by the CG method may be viewed as the problem of minimizing a twice continuously differentiable and non-quadratic function. Papadrakakis and Gantes [6] applied this procedure to truncate the Newton–Raphson method. For further details about this method, interested readers could refer to reference [6].

4.3. Proposed HPM for the nonlinear analysis

In this section, a newly developed approach based on HPM is described for solution of nonlinear equations. The method is applied to the nonlinear analysis of plane frames. As mentioned before, the HPM approach appears to be an attractive tool for solving of nonlinear equations systems. In this method, a nonlinear system of equations is transformed to a series of linear and nonlinear parts. These sets of equations are then solved iteratively. Finally, a linear series of the solutions completes the answer if convergence has reached. In the following, the development of new formulation for solving nonlinear equation systems is described. It is followed by introduction of an algorithm developed for solution of nonlinear problems especially for analysis of planar frames. This algorithm can be used to improve a nonlinear analysis which is based on displacement control method.

Consider a series of n nonlinear equation $g_{1(x)}, g_{2(x)}, \ldots\ldots, g_{n(x)}$ with n variable $x_1, x_2, \ldots\ldots, x_n$ such that:

$$\left\{g_{(x)}\right\} = 0 \tag{18}$$

in which

$$\{x\} = \{x_1, \ldots, x_n\}^T \tag{19}$$

$$\left\{g_{(x)}\right\} = \left\{g_{(x_1)}, \ldots, g_{(x_n)}\right\}^T. \tag{20}$$

If, respectively, x^* and w be the exact solution of system of equations and the initial guess, Taylor series can be used to expand Eq. (18) as follows:

$$\left\{g_{(x)}\right\} = \left\{g_{(w)}\right\} + \left[J_{(w)}\right](\{x\} - \{w\}) + \left\{G_{(x)}\right\} = 0 \tag{21}$$

where $\{G_{(x)}\}$ is defined by the following relation:

$$\left\{G_{(x)}\right\} = \left\{g_{(x)}\right\} - \left\{g_{(w)}\right\} - \left[J_{(w)}\right](\{x\} - \{w\}) \tag{22}$$

and $[J_{(x)}]$ is a Jacobin matrix in which J_{ij} is positioned at ith row and jth column and is mathematically described by the following relation:

$$J_{ij} = \frac{\partial g_i}{\partial x_j}. \tag{23}$$

The following equation can then be solved for $\{x\}$:

$$\{x\} = \{w\} - \left[J_{(w)}\right]^{-1}\left(\left\{g_{(w)}\right\} + \left\{G_{(x)}\right\}\right). \tag{24}$$

To reach approximate solution for $\{x\}$from Eq. (24), Homotopy is first shaped:

$$H(\bar{x}, p) = \{\bar{x}\} - \{w\} - \left[J_{(w)}\right]^{-1}\left(\left\{g_{(w)}\right\} + p\left\{G_{(\bar{x})}\right\}\right) = 0. \tag{25}$$

In which p number is a coefficient that varies within a range 0 through 1. In special case of $p = 0$, Eq. (25) is reduced to:

$$H(\bar{x}, 0) = \{\bar{x}\} - \{w\} - \left[J_{(w)}\right]^{-1}\left\{g_{(w)}\right\} = 0. \tag{26}$$

On the other hand, if p is assigned unity, $p = 1$, Eq. (25) is defined by:

$$H(\bar{x}, 1) = \{\bar{x}\} - \{w\} - \left[J_{(w)}\right]^{-1}\left(\left\{g_{(w)}\right\} + \left\{G_{(\bar{x})}\right\}\right) = 0. \tag{27}$$

In the latter situation, $\{\bar{x}\}$ will be equal to $\{x^*\}$ which further implies that exact solution has been reached. The answer to the Eq. (25) can be obtained as:

$$\{\bar{x}\} = \{x_0\} + p\left\{x_1^{\,1}\right\} + p^2\{x_2\} + \ldots \tag{28}$$

In follows that solution of Eq. (24) may be reached if the following relation is used:

$$\{x_*\} = \lim_{p \to 1}\{\bar{x}\} = \{x_0\} + \{x_1\} + \{x_2\} + \ldots \tag{29}$$

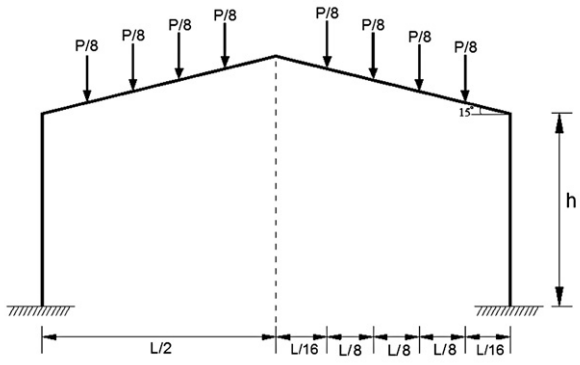

Fig. 5. Structure's geometry example 1.

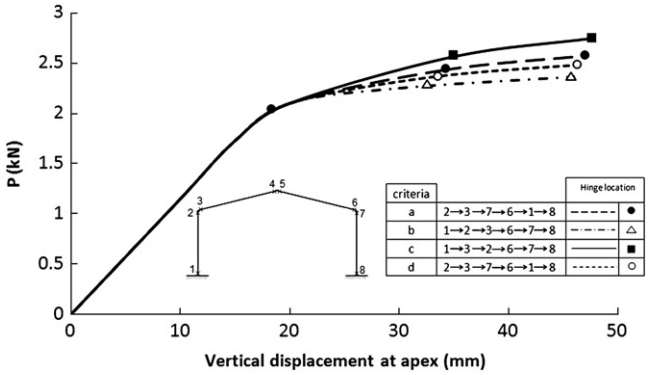

Fig. 6. Load–deflection curve for example 1.

Substituting Eq. (28) into Eq. (25) and using Taylor series of $\{G_{(x)}\}$ around$\{x_0\}$ one obtains [24]:

$$\{x_0\}+p\{x_1\}+p^2\{x_2\}\ldots=\{w\}+\left[J_{(w)}\right]^{-1}\left\{g_{(w)}\right\} +p\left[J_{(w)}\right]^{-1}\left(\left\{G_{(x_0)}\right\}+\left[J_{(x_0)}\right]^{-1}\left(p\{x_1\}+p^2\{x_2\}+\ldots\right)\right)=0. \tag{30}$$

In Eq. (30) coefficients of different powers for p in both sides of relation is considered which results in:

$$\{x_0\}=\{w\}-\left[J_{(w)}\right]^{-1}\left\{g_{(w)}\right\} \tag{31}$$

$$\{x_1\}=-\left[J_{(w)}\right]^{-1}\left\{G_{(x_0)}\right\} \tag{32}$$

$$\{x_2\}=-\left[J_{(w)}\right]^{-1}\left(\left[J_{(x_0)}\right]\{x_1\}\right). \tag{33}$$

If relations (31, 32, 33) are substituted into Eq. (29), the following relation is reached:

$$\{x_*\}=\{w\}-\left[J_{(w)}\right]^{-1}\left\{g_{(w)}\right\}-\left[J_{(w)}\right]^{-1}\left\{G_{(x_0)}\right\}-\left[J_{(w)}\right]^{-1}\left(\left[J_{(x_0)}\right]\{x_1\}\right)+\ldots \tag{34}$$

which can be further simplified as:

$$\{x_*\}=\{w\}+\left[J_{(w)}\right]^{-1}\left\{g_{(w)}\right\}+\left[J_{(w)}\right]^{-1}G_{\left(\{w\}+\left[J_{(w)}\right]^{-1}\{g(w)\}\right)}+\ldots \tag{35}$$

Eq. (35) can be written alternatively in the following form:

$$\{x_*\}-\{w\}\approx\left[J_{(w)}\right]^{-1}\left\{g_{(w)}\right\}+\left[J_{(w)}\right]^{-1}G_{\left(\{w\}+\left[J_{(w)}\right]^{-1}\{g(w)\}\right)}. \tag{36}$$

Substituting G from Eq. (22) into Eq. (36) yields:

$$\{x_*\}-\{w\}\approx-\left[J_{(w)}\right]^{-1}\left\{g_{(w)}\right\}+\left[J_{(w)}\right]^{-1}\left\{g_{\left(w+\left[J_{(w)}\right]^{-1}\{g(w)\}\right)}\right\}. \tag{37}$$

Table 1
Corresponding displacements (mm) obtained by current and other methods in example 1.

Load (kN)	Newton–Raphson [26]	Conjugate gradient	Homotopy perturbation	Finite element (OpenSees)
0.5	5.16748	5.16748	5.16748	5.16746
1.15	10.19125	10.19124	10.19125	10.19123
1.725	15.1322	15.13222	15.13221	15.13215
2.1	20.05175	20.05176	20.05174	20.05161
2.3625	33.0642	33.06418	33.06419	33.06396
2.5	48.05459	48.05457	48.05458	48.05443

Table 2
Comparison of CPU time and number of iterations for the methods used in example 1.

Newton–Raphson method		CG method		Present study	
No. of iterations	Time (s)	No. of iterations	Time (s)	No. of iterations	Time (s)
83	4.25	70	1.89	64	1.62

The above relation can be used for solving the system of nonlinear equilibrium equation which is explained in the next section.

4.4. Implementation of HPM in structural engineering

To carry out HPM, a computer program has been developed using MATLAB codes and representative results are provided in the following. The new approach introduced in this paper is examined for four yield criteria, discussed earlier, i.e. Eqs. (14) thru (17).

Consider the following relation to be applied to Eq. (20):

$$\left\{g_{(x)}\right\}=\{P\}-\left\{f_{(x)}\right\} \tag{38}$$

in which vector $\{x\}$ includes generalized coordinates and is formed by nodal translations, $\{f\}$ is resultant vector of internal forces, and $\{P\}$ is vector of external forces. The Jacobian matrix is defined as:

$$\left[J_{(x)}\right]=-[\tau] \tag{39}$$

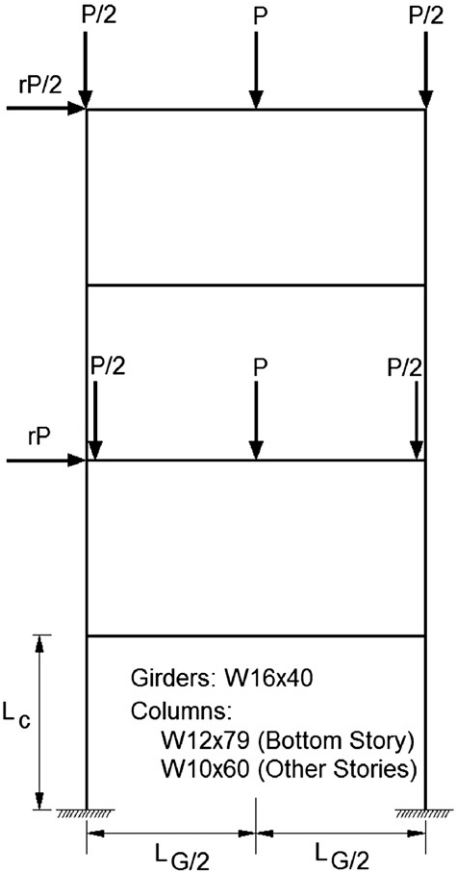

Fig. 7. Structure's geometry example 2.

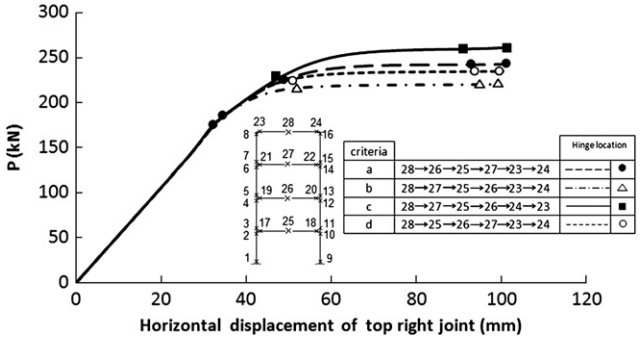

Fig. 8. Load–deflection curve for example 2.

where $[\tau]$ is tangent stiffness matrix. Therefore Eq. (37) can be expressed as follows:

$$\{\Delta x\} \approx [\tau]^{-1}\left\{P - f_{(x)}\right\} + [\tau]^{-1}\left(\{P\} - \left\{f_{\left(x+[\tau]^{-1}\{P-f_{(x)}\}\right)}\right\}\right). \tag{40}$$

Numerical implementation of Eq. (40) requires assuming an initial and approximate solution similar to that applies to Newton–Raphson method. According to above formulation a new iterative algorithm is introduced for nonlinear analysis using HPM. The proposed algorithm includes the following major steps:

Step 1) Initialize variables, parameters, and input incremental load, $\{\Delta P\}$.

Step 2) Input joint coordinates, connectivity, boundary conditions, and material properties.

Step 3) Establish the member tangent stiffness matrix $[T]$ and then assemble it into the system tangent stiffness matrix $[\tau]$.

Step 4) For 1st iteration in $(i+1)$th loading step, calculate incremental displacement, $\{\Delta x\}_1^{i+1}$ as:

$$\{\Delta x\}_1^{i+1} = \left[\tau^1\right]_{i+1}^{-1} \{\Delta P\}^{i+1}. \tag{41}$$

Step 5) Update the nodal coordinates based on the following relation:

$$\{x\}_1^{i+1} = \{x\}^i + \{\Delta x\}_1^{i+1}. \tag{42}$$

Step 6) Determine the unbalanced forces in jth iteration (or 1st iteration) and $(i+1)$th loading step $\{\Delta Q\}_j^{i+1}$:

$$\{\Delta Q\}_j^{i+1} = \{P\}^{i+1} - \left\{f_{\left(x_j^{i+1}\right)}\right\} \tag{43}$$

Table 3
Corresponding displacements (mm) obtained by current and other methods in example 2.

Load (kN)	Newton–Raphson [2]	Conjugate gradient	Homotopy perturbation	Finite element (OpenSees)
100	8.65201	8.65201	8.65201	8.65199
175	15.34130	15.34131	15.34131	15.34129
216	19.33065	19.33067	19.33066	19.33060
230	25.78136	25.78134	25.78135	25.78126
238	35.81166	35.81166	35.81167	35.81157
245	44.14087	44.14089	44.14088	44.14079

Table 4
Comparison of CPU time and number of iterations for example 2.

Newton–Raphson method		CG method		Present study	
No. of iterations	Time (s)	No. of iterations	Time (s)	No. of iterations	Time (s)
96	3.04	80	1.72	72	1.46

Step 7) Calculate $\{\Delta x_j^{i+1}\}$ using relations shown below:

$$\begin{aligned} \{\Delta x\}_{j0}^{i+1} &= \left[\tau^j\right]_{i+1}^{-1} \{\Delta Q\}_j^{i+1} \\ \{\Delta x\}_j^{i+1} &= \{\Delta x\}_{j0}^{i+1} + \left[\tau^j\right]_{i+1}^{-1} \left\{P^{i+1} - f_{\left(x_j^{i+1} + \Delta x_{j0}^{i+1}\right)}\right\}. \end{aligned} \tag{44}$$

Step 8) Update joint geometry:

$$\left\{x_j^{i+1}\right\} = \left\{x_{j-1}^{i+1}\right\} + \left\{\Delta x_j^{i+1}\right\}. \tag{45}$$

Step 9) Repeat step 6 through 8 until the convergence criterion is satisfied within predefined tolerance:

$$\sqrt{\frac{\sum_i (\Delta x_i)^2}{\sum_i (x_i)^2}} \le e. \tag{46}$$

in which e is the error tolerance.

Step 10) Apply next load increment $\{\Delta P\}$ and return to step 1.

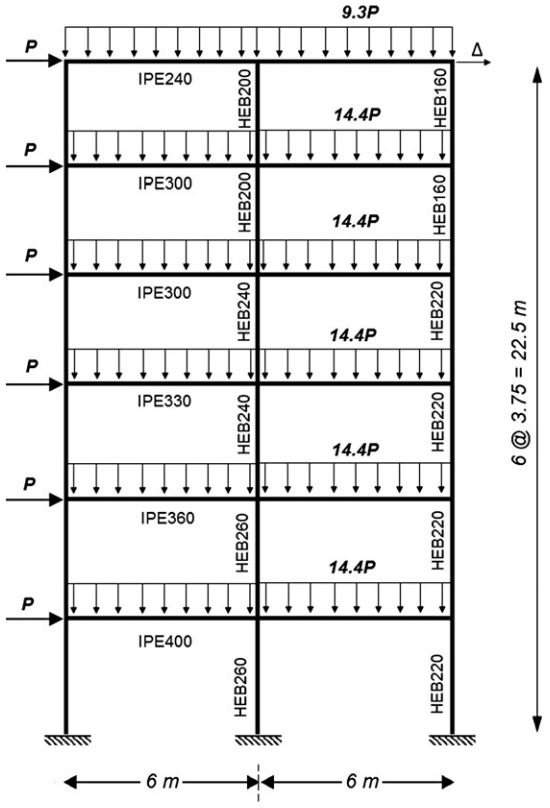

Fig. 9. Two-bay six-storey frame.

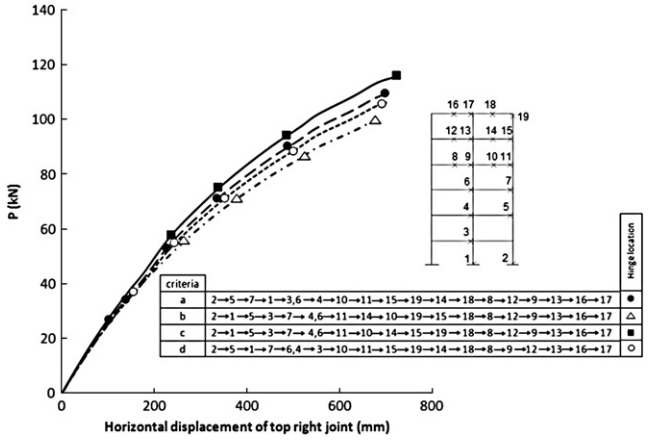

Fig. 10. Load–deflection curve for example 3.

5. Numerical examples

The efficiency and applicability of the procedure presented in preceding sections is evaluated in this section. Numerical examples are presented and are solved using the current approach, CG method, and also by Newton–Raphson method. Also, the results of these methods are compared with those given by finite element method. For this purpose, OpenSees software [25] which is an object-oriented framework for finite element analysis is used for modeling of structures.

Examples discussed and solved include four types of planar frames. Results obtained are considered and, in particular, the rates of convergence and calculation time are compared. A predefined tolerance of 10^{-3} is also assigned to all methods used in the analysis.

Four yield criteria as those discussed in Section 3 are employed in the analysis in order to increase the level of sophistication, generality, and applicability of the method presented here.

5.1. Example 1

The first example concerns a pitched roof frame shown in Fig. 5 [26]. Let $EI = 460748$ kN.mm^2, $L = 1219$ mm, $h = 406$ mm, $A = 169$ mm^2 and $M_p = 153.793$ kN.mm, the external loading was equipment loading which consists of P and $\Delta P = 0.238$ kN.

The sequences of plasticization for the frame analyzed are shown in its load–deflection curve (Fig. 6). The results (Fig. 6 "*d*" yield criterion) are compared with those given by reference [26] and finite element method (OpenSees) in Table 1 which shows all methods are tightly closed together.

An investigation into the results shown in Table 2 clearly implies on the efficiency of the current approach when compared with classic Newton–Raphson and CG methods. Particularly, in Newton–Raphson method the number of iterations and computational time to reach convergence are respectively 22% and 46% higher the current approach.

Table 5
Corresponding displacements (mm) obtained by current and other methods in example 3.

Load (kN)	Newton–Raphson [22]	Conjugate gradient	Homotopy perturbation	Finite element (OpenSees)
16.352	61.84030	61.84030	61.84030	61.84028
34.748	145.13121	145.13122	145.13121	145.13117
51.165	224.26367	224.26366	224.26365	224.26361
70.825	348.85954	348.85955	348.85953	348.85947
90.140	514.92587	514.92589	514.92588	514.92578
107.310	725.09757	725.09755	725.09756	725.09748

Table 6
Comparison of CPU time and number of iterations for example 3.

Newton–Raphson method		CG method		Present study	
No. iteration	Time (s)	No. iteration	Time (s)	No. iteration	Time (s)
162	19.62	129	11.53	117	9.01

5.2. Example 2

A four-storey frame, shown in Fig. 7 is adopted in this example similar to that analyzed in reference [2]. Selecting such an example provides possibility of comparing results obtained by three different approaches. The engineering properties of the frame members are given as follows: $L_C = 3.66$ m, $L_G = 9.15$ m, $E = 201 \times 10^6$ kPa, $F_y = 236 \times 10^3$ kPa. The value of the lateral load parameter, r, is equal to 0.1, increment of load $\Delta P = 5$ kN.

Fig. 8 illustrates load–deflection responses obtained from the proposed formulation and sequence of plasticization base on four yield criteria adopted for the nonlinear analysis. From the equilibrium path (yield criterion "*d*" adopted among others shown in Fig. 8), six points are selected and their load–displacement coordinates are extracted and listed in Table 3 correspondingly. This table includes also results obtained in reference [22] and finite element method (OpenSees) which makes a base for further comparison.

Table 4 presents a summary on the performance of the methods applied, including present approach, to the problem raised in example 2. The results show that in HPM the number of iterations has reduced to 25% while computational time has also declined to 52% compared with Newton–Raphson method.

5.3. Example 3

Fig. 9 shows a two-bay six-storey frame subjected to distributed gravity and lateral loads. The selected types of beam and column members are shown in the figure while all loading magnitudes are scaled to a reference and predefined value of P [22]. The elastic modulus for all members E is adopted as 20500 kN/cm^2. Incremental load (ΔP) is selected equal to 2.044 kN.

The sequence of plasticization for the six-storey frame are shown in Fig. 10. The results (Fig. 10 "*d*" yield criterion) are compared with those given by reference [22] and finite element method (OpenSees) in Table 5 which shows all methods are tightly closed together.

The efficiency and performance of the HPM can be deduced from the results shown in Table 6.

As can be seen in the table, when proposed HPM is used the number of iterations and computational time is reduced compared with those taken by Newton–Raphson and CG methods. In particular, in the current example, the rates of reduction in the number of iterations and computing time are up to 28% and 54% respectively when compared with the classic Newton–Raphson method. Therefore, the proposed method is of practical interest whenever the accuracy and efficiency are both concerned in the nonlinear analysis of structures.

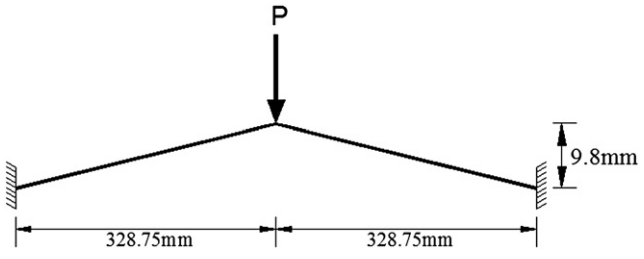

Fig. 11. The William's toggle-frame.

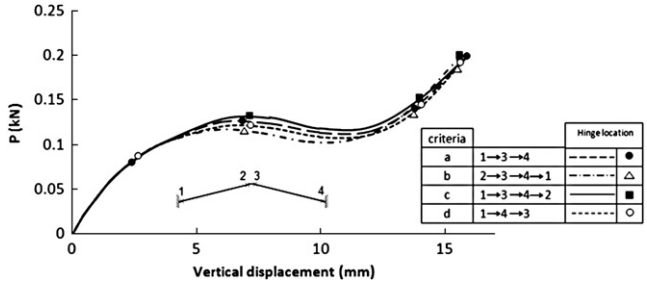

Fig. 12. Load–deflection curve for example 4.

5.4. Example 4

Fig. 11 shows the well-known William's toggle frame consisting of two members under a vertical load P [27]. The following properties have been assumed for each member of frame: $E = 71 \times 10^6$ kPa, $A = 1.18$ cm^2, $I = 0.0375$ cm^4.

Fig. 12 shows the variation of vertical displacement with the load P. Table 7 constitutes the results (Fig. 12 "d" yield criterion) obtained from current approach and finite element method. The table clearly shows the accuracy of the current method (HPM) as well as those presented in reference [27] and makes a good basis for further comparison.

To compare the performance of the current HPM, the results of analyses are summarized in Table 8. The computations are carried out with a high precision. It can be easily seen that less number of iterations and computational time are used by homotopy technique developed in this study. For this last example, the Newton–Raphson method's computational time and number of iterations to reach convergence are respectively 59% and 37% higher than those taken by current approach.

6. Conclusions

This paper presented an advanced numerical scheme to reduce the computation time and number of iterations required to converge for the equilibrium path in the geometric and material non-linearity analysis of steel plane frames. The main object was to develop a more efficient implementation procedure for employment of iterative methods. A mathematical formulation, known as Homotopy Perturbation Method, was numerically extended and applied for nonlinear analysis of plane frames. A particular algorithm was written associated with computer codes for programming and implementation by microcomputers. Sequence of plasticization occurred in some sample structures were exemplified and the results obtained were compared for various types of steel element yield criteria. It was shown that HPM needs less computational effort such that, both number of iterations and computational time for analysis was reduced, in particular when compared with classic Newton–Raphson method. The method is, therefore, a powerful numerical scheme and is an efficient technique for geometric and material non-linearity analysis of structures.

Table 7
Corresponding displacements (mm) obtained by current and other methods in example 4.

Load (kN)	Newton–Raphson [27]	Conjugate gradient	Homotopy perturbation	Finite element (OpenSees)
0.02001	0.44795	0.44795	0.44795	0.44794
0.08006	2.34798	2.34799	2.34798	2.34791
0.12013	5.91519	5.91518	5.91517	5.91509
0.10869	9.92547	9.92546	9.92548	9.92538
0.14011	13.93553	13.93555	13.93553	13.93547
0.20016	15.94228	15.94228	15.94227	15.94221

Table 8
Comparison of CPU time and number of iterations for example 4.

Newton–Raphson method		CG method		Present study	
No. of iterations	Time (s)	No. of iterations	Time (s)	No. of iterations	Time (s)
54	1.23	39	0.59	34	0.50

References

[1] Abbasnia R, Kassimali A. Large deformation elastic–plastic analysis of space frames. J Constr Steel Res 1995;35:275–90.
[2] Kassimali A. Large deformation analysis of elastic–plastic frames. ASCE J Struct Eng 1983;109:1869–86.
[3] Kassimali A, Abbasnia R. Large deformation analysis of elastic space frames. ASCE J Struct Eng 1991;117:2069–87.
[4] Haisler WE, Stricklin JA, Stebbins FJ. Development and evaluation of solution procedures for geometrically nonlinear structural analysis. AIAA J 1972;10:264–72.
[5] Massett DA, Stricklin JA. Self-correcting incremental approach in nonlinear structural mechanics. AIAA J 1971;9:2464–6.
[6] Papadrakakis M, Gantes CJ. Truncated Newton methods for nonlinear finite element analysis. Comput Struct 1988;30:705–14.
[7] Saffari H, Fadaee MJ, Tabatabaei R. Nonlinear analysis of space trusses using modified normal flow algorithm. ASCE J Struct Eng 2008;134:998–1005.
[8] Papadrakakis M. Post-buckling analysis of spatial structures by vector iteration methods. Comput Struct 1981;14:393–402.
[9] Crisfield MA. Non-linear finite element analysis of solids and structures. England: John Wiley; 1991.
[10] Saffari H, Mansouri I. Non–linear analysis of structures using two–point method. Int J Non–Linear Mech 2011;46:834–40.
[11] Tabatabaei R, Saffari H, Fadaee MJ. Application of normal flow algorithm in modal adaptive pushover analysis. J Constr Steel Res 2009;65:89–96.
[12] Dai SQ, et al. Top 10 progress of theoretical and applied mechanics in the 20th century. Adv Mech 2001;31:322–6.
[13] Liao SJ. The proposed homotopy analysis technique for the solution of nonlinear problems. Ph.D. Thesis, Shanghai Jiao Tong University, Shanghai: China; 1992.
[14] Liao SJ. Beyond perturbation: introduction to the homotopy analysis method. Boca Raton: Chapman & Hall/CRC Press; 2003.
[15] Chow SN, Mallet-Paret J, Yorke JA. Finding zeros of maps: homotopy methods that are constructive with probability one. Math Comput 1978;32:887–99.
[16] Watson LT. Solving finite difference approximations to nonlinear two-point boundary value problems by a homotopy method. SIAM J Sci Statist Comput 1980;1:467–80.
[17] Wang X, Li TY. Nonlinear homotopies for solving deficient polynomial system with parameter. SIAM J Numer Anal 1992;29:1104–18.
[18] Golbabai A, Javidi M. Newton-like iterative methods for solving system of non-linear equations. Appl Math Comput 2007;192:546–51.
[19] Oran C. Tangent stiffness in plane frames. ASCE J Struct Eng Div 1973;99:973–85.
[20] Spiliopoulos KV, Patsios TN. An efficient mathematical programming method for the elastoplastic analysis of frames. Eng Struct 2010;32:1199–214.
[21] Load and resistance factor design specification for structural steel buildings. 2nd ed. Chicago: American Institute of Steel Construction; 1993.
[22] Chan SL, Chui PPT. Non-linear static and cyclic analysis of steel frames with semi-rigid connections. 1st ed. The Netherlands: Elsevier Science; 2000.
[23] McGuire W, Gallagher RH, Ziemian RD. Matrix structural analysis. 2nd ed. USA: John Wiley; 2000.
[24] He JH. Homotopy perturbation technique. Comput Meth Appl Mech Eng 1999;178:257–62.
[25] Mazzoni S, McKenna F, Scott MH, Fenves GL. Open system for earthquake engineering simulation (OpenSees), user command-language manual. University of California: Berkeley (CA): Pacific Earthquake Engineering Research. PEER; 2007.
[26] Majid KI. Non-linear structures. New York, N.Y.: John Wiley and Sons, Inc.; 1972
[27] Yang YB, Kuo SR. Theory and analysis of nonlinear framed structures. 1st ed. Singapore: Prentice Hall PTR; 1994.